



Universiteit  
Leiden  
The Netherlands

## Synthetic studies with bacitracin A and preparation of analogues containing alternative zinc binding groups

Buijs, N.; Vlaming, H.C.; Haren, M.J. van; Martin, N.I.

### Citation

Buijs, N., Vlaming, H. C., Haren, M. J. van, & Martin, N. I. (2022). Synthetic studies with bacitracin A and preparation of analogues containing alternative zinc binding groups. *Chembiochem*, 23(24). doi:10.1002/cbic.202200547

Version: Publisher's Version

License: [Creative Commons CC BY-NC-ND 4.0 license](https://creativecommons.org/licenses/by-nc-nd/4.0/)

Downloaded from: <https://hdl.handle.net/1887/3515157>

**Note:** To cite this publication please use the final published version (if applicable).

# Synthetic Studies with Bacitracin A and Preparation of Analogues Containing Alternative Zinc Binding Groups

Ned Buijs,<sup>[a]</sup> Halana C. Vlaming,<sup>[a]</sup> Matthijs J. van Haren,<sup>[a]</sup> and Nathaniel I. Martin<sup>\*[a]</sup>

The growing threat of drug-resistant bacteria is a global concern, highlighting the urgent need for new antibiotics and antibacterial strategies. In this light, practical synthetic access to natural product antibiotics can provide important structure-activity insights while also opening avenues for the development of novel analogues with improved properties. To this end, we report an optimised synthetic route for the preparation of the clinically used macrocyclic peptide antibiotic bacitracin. Our

combined solid- and solution-phase approach addresses the problematic, and previously unreported, formation of undesired epimers associated with the stereochemically fragile N-terminal thiazoline moiety. A number of bacitracin analogues were also prepared wherein the thiazoline motif was replaced by other known zinc-binding moieties and their antibacterial activities evaluated.

## Introduction

The accelerating appearance of antimicrobial resistance (AMR) is a growing global public health risk. In 2019 nearly 1.3 million deaths could be directly attributed to AMR.<sup>[1]</sup> Despite the increasing need for new antibacterial agents, only two mechanistically novel classes of antibiotics have been approved in the last 40 years, namely, linezolid and daptomycin.<sup>[2]</sup> As the prevalence of multi-drug resistant bacteria grows, the need to develop new and more potent antibacterial agents is greater than ever.<sup>[3]</sup> In this light, natural product antibiotics remain a rich source of structural and mechanistic diversity. One such example is bacitracin which comprises a family of structurally similar macrocyclic peptides, the most well-known of which is bacitracin A (1, Figure 1A).<sup>[4]</sup> Produced by strains of *Bacillus licheniformis* and *Bacillus subtilis*, bacitracin exhibits activity against Gram-positive bacteria.<sup>[5]</sup> The moderate activity and systemic toxicity of bacitracin A have restricted its use to topical applications, where it is often formulated along with neomycin and polymyxin B, for the treatment of minor cuts and burns.<sup>[5–6]</sup> Notably, while bacitracin has been used widely in both the pharmaceutical and livestock industries for over 70 years, little occurrence of resistance has been reported during this time.<sup>[7]</sup>

Structurally, bacitracin A is a 12-mer macrocyclic peptide consisting of both L- and D-amino acids, and is biosynthesised by a dedicated nonribosomal peptide synthetase.<sup>[8]</sup> The macrocycle is formed via an amide linkage between the side chain of

Lys6 and the peptide C-terminus. The N-terminus of bacitracin A contains an unusual aminothiazoline motif generated by the enzymatic condensation of L-cysteine and L-isoleucine.<sup>[7]</sup> The N-terminal amine is critical for antibiotic activity given that bacitracin F, a degradation product of bacitracin A formed by the oxidative deamination of the aminothiazoline to give the corresponding ketothiazole, is inactive (see Supporting Scheme S1).<sup>[4,9]</sup> Notably, bacitracin F is reported to be nephro-

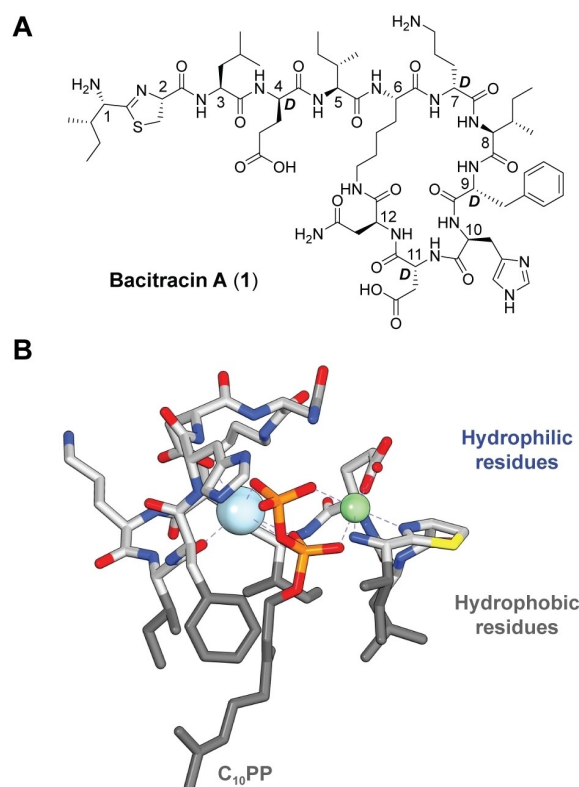


**Figure 1.** (A) Structure of Bacitracin A (1). (B): Crystal structure of bacitracin A complexed with geranyl-pyrophosphate mediated by  $Zn^{2+}$  (green) and  $Na^+$  (light blue). Adapted from PDB ID: 4 K7T.<sup>[14]</sup>

[a] N. Buijs, H. C. Vlaming, M. J. van Haren, N. I. Martin  
Biological Chemistry Group  
Institute of Biology Leiden, Leiden University  
Sylviusweg 72, 2333 BE, Leiden (The Netherlands)  
E-mail: n.i.martin@biology.leidenuniv.nl

Supporting information for this article is available on the WWW under <https://doi.org/10.1002/cbic.202200547>

© 2022 The Authors. ChemBioChem published by Wiley-VCH GmbH. This is an open access article under the terms of the Creative Commons Attribution Non-Commercial NoDerivs License, which permits use and distribution in any medium, provided the original work is properly cited, the use is non-commercial and no modifications or adaptations are made.

toxic and its formation *in vivo* limits the systemic applications of bacitracin.<sup>[6]</sup> Mechanistically, bacitracin functions in a manner distinct from all other antibiotics that target bacterial cell wall biosynthesis. Specifically, in the presence of a divalent metal ion, most commonly  $Zn^{2+}$ , bacitracin binds to and sequesters the membrane-associated phospholipid isoprenyl pyrophosphate ( $C_{55}PP$ ).<sup>[10,11]</sup> Given that  $C_{55}PP$  does not play a role in mammalian cell metabolism, it presents a target unique to bacteria with great promise for antibiotic development.<sup>[11,12]</sup>

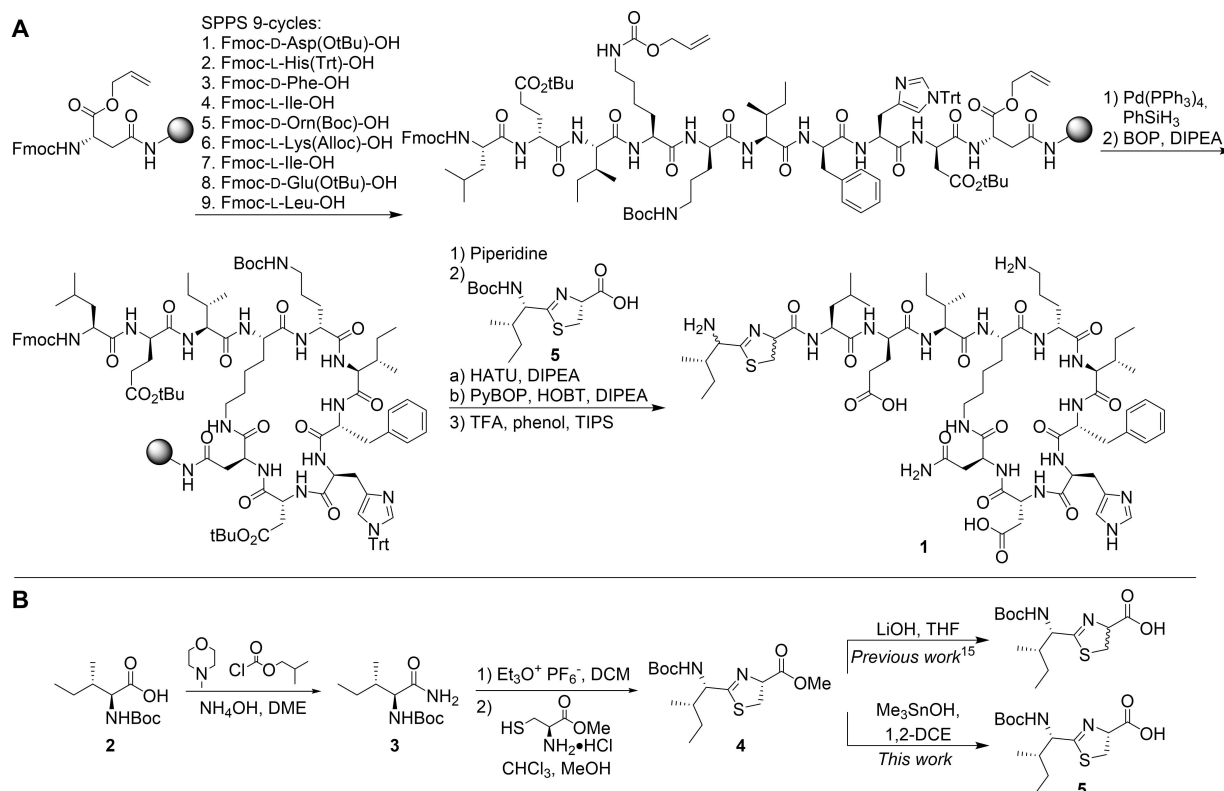
Recent structural studies by Loll and co-workers revealed that bacitracin forms a well-defined ternary 1:1:1 antibiotic- $Zn^{2+}$ -lipid complex (along with a flanking  $Na^+$  ion) clearly illustrating how  $C_{55}PP$  is bound while also explaining the  $Zn^{2+}$ -dependence of bacitracin's antibiotic activity (Figure 1B).<sup>[13,14]</sup> Also of note is the finding that in the context of the ternary complex, the side chains of the hydrophobic residues at positions 1, 3, 5, 8, and 9 align to form a face that presumably interacts with the bacterial membrane, while the polar side chains of residues 2, 4, 7, 10, 11, and 12 are in turn exposed to the aqueous environment.

The combination of bacitracin's unique mechanism of action and low incidence of resistance, as well as the structural limitations that prevent its wider clinical application, make it an appealing scaffold for variation. This prompted us to undertake investigations into the synthesis of bacitracin A with the goal of generating novel analogues that maintain the unique antibiotic activity of the parent compound while also addressing its structural liabilities. We here report an optimised route for the

synthesis of bacitracin that was in turn used to generate a number of bacitracin analogues wherein the thiazoline moiety was replaced with other zinc-binding motifs.

## Results and Discussion

The solid-phase total synthesis of Bacitracin A was first reported by Griffin and co-workers in 1996<sup>[15]</sup> and we began our investigation by attempting to reproduce the published synthesis (Scheme 1). This commenced with rink amide resin loaded with an allyl protected aspartic acid building block coupled via its side chain carboxylate (corresponding to the C-terminal Asn12 residue) after which nine successive Fmoc-SPPS cycles were applied to yield the linear decapeptide intermediate. Of note, installation of the residue corresponding to Lys6 was performed using Fmoc-Lys(Alloc)-OH. Subsequent on-resin treatment of the peptide with  $Pd(PPh_3)_4$  led to the simultaneous removal of the Alloc and Allyl ester groups at Lys6 and Asn12 respectively. The partially protected peptide was then treated with BOP/DIPEA, which smoothly mediated the formation of the peptide macrocycle. As shown in Scheme 1, the next step in the synthesis called for coupling of Boc-protected aminothiazoline building block 5. However, our attempts at reproducing the synthesis of thiazoline dipeptide 5 were plagued by racemisation of the thiazoline stereocentre during the final saponification step (Scheme 1B). While the methyl ester precursor 4 was cleanly formed in high stereochemical purity, in our hands the



**Scheme 1.** (A) Synthesis of bacitracin A with reported thiazoline coupling conditions.<sup>[15]</sup> (B) Optimised synthesis of thiazoline carboxylic acid 5.

reported hydrolysis conditions employing LiOH consistently generated a mixture of diastereomers. Attempted separation of the diastereomers by means of silica gel column chromatography only made matters worse as further stereochemical scrambling was found to occur under these conditions. While no mention of this issue was included in the 1996 publication, recent reports describing the synthesis of structurally similar thiazoline containing carboxylic acids do make note of their propensity to epimerise under a variety of conditions.<sup>[16]</sup> After exploring a number of options, we were pleased to find that this issue could be overcome by applying a mild and selective method for hydrolysing methyl esters previously reported by the Nicolaou group.<sup>[17]</sup> Specifically, treatment of thiazoline methyl ester **4** with trimethyltin hydroxide led to complete conversion within two hours, after which a convenient aqueous workup to remove tin salts providing the desired product in a purity suitable to avoid the need for silica chromatography (Scheme 1B).

With access to the amino thiazoline carboxylic acid **5** in stereochemically pure form, the synthesis of bacitracin A was continued. To this end, we applied the previously described conditions employing a double coupling of **5**, first with HATU, then with PyBOP/HOBt, to the resin-bound peptide macrocycle. However, following resin cleavage and global deprotection by treatment with TFA, LC-MS analysis indicated the presence of four peaks of similar intensity and all with the same mass as bacitracin A, which we subsequently labelled BacA<sub>A-D</sub>, based on the order in which they eluted (Figure S1). Notably, BacA<sub>D</sub> (the last eluting species) was found to have the same retention time as bacitracin A obtained from commercial sources (Figure S2). These findings led us to surmise that four diastereomeric species are formed as a result of the activation of **5** in the presence of base, which can cause epimerisation of the  $\alpha$ -position, along with the subsequent TFA treatment, which in turn can cause scrambling of the isoleucine  $\alpha$ -position (see Scheme S2 for proposed mechanism of base- and acid-mediated epimerisation). While not mentioned in the original bacitracin synthesis, such pathways are in line with other reports describing the susceptibility of bacitracin's thiazoline moiety, and thiazolines in general, to racemisation.<sup>[16,18–20]</sup>

To evaluate the antibacterial properties of the different bacitracin diastereomers, the four species were first separated using preparative HPLC. The antibacterial activities of BacA<sub>A-D</sub> were assessed in a minimum inhibitory concentration (MIC) assay run against a panel of representative Gram-positive

bacterial strains. Of note, the media used in the MIC assay was supplemented with 0.3 mM ZnSO<sub>4</sub> to provide the divalent metal ion required for bacitracin's activity.<sup>[21]</sup> The activity of the four BacA<sub>A-D</sub> diastereomers was compared to that of commercially sourced bacitracin A as well as vancomycin, which served as a positive control. The results of the MIC assay are summarized in Table 1 and reveal that of the four diastereomers, BacA<sub>D</sub> matches the potency of the natural product, a result in keeping with the co-elution study (Figure S2), while the other three diastereomers all exhibit significantly reduced antimicrobial activity. Based on these results it was concluded that the BacA<sub>D</sub> diastereomer corresponds to the natural product. To further confirm this we next turned to NMR spectroscopy wherein both 1- and 2-D NMR experiments revealed the spectra of the BacA<sub>D</sub> diastereomer to be identical to that of bacitracin A (Figures S3–S4, Table S1–S2).

In an attempt to optimise the synthesis of bacitracin we turned our attention to minimising the formation of the unwanted diastereomers associated with the stereochemical scrambling of the aminothiazoline moiety. To do so, we first investigated the acidic conditions used for resin cleavage and global deprotection. As noted above, we suspected that under acidic conditions the  $\alpha$ -position of the N-terminal Ile residue involved in the aminothiazoline moiety could be prone to racemization. In fact, the capacity for acid treatment of bacitracin A to cause formation of a "low potency" isomeric form of bacitracin was first reported in 1961 by Konigsberg et al.<sup>[22]</sup> To further explore this phenomenon we therefore treated commercially sourced, pure bacitracin A with the same acidic cleavage cocktail (95:2.5:2.5 TFA/TIPS/H<sub>2</sub>O) used in the final SPPS step. This study revealed that under these conditions bacitracin A converts to a new species with the same mass and a retention time corresponding to the BacA<sub>B</sub> diastereomer previously isolated (Figure S5). Notably, this was found to be a time-dependent process resulting in near complete epimerisation after 2 hours while at 30 minutes epimerisation was assessed to be > 15%. Given this insight, we therefore opted to use a 30-minute cleavage in our subsequent bacitracin syntheses, which facilitated > 95% deprotection while effectively minimising epimerisation at the Ile1 position.

We next examined the conditions used for activation and coupling thiazoline building block **5** to the resin-bound peptide. As also previously mentioned, the stereochemical integrity of the  $\alpha$ -position corresponding to Cys2 of the thiazoline motif was found to be very susceptible to basic conditions. In

**Table 1.** Minimum inhibition concentration (MIC) values for bacitracin A diastereomers compared with natural bacitracin A and vancomycin.

Compound	MIC <sup>[a]</sup>				
	<i>S. aureus</i> ATCC 29213 (MSSA)	<i>S. aureus</i> USA300 (MRSA)	<i>B. subtilis</i> 168	<i>S. simulans</i> 22	<i>E. faecium</i> E980
BacA <sub>A</sub>	> 64	> 64	> 64	8	> 64
BacA <sub>B</sub>	16	16	64	1	32
BacA <sub>C</sub>	> 64	> 64	> 64	2	> 64
BacA <sub>D</sub>	2	2	32	0.25	16
Bacitracin A (commercial)	2	2	32	0.25	16
Vancomycin	1	2	0.25	0.5	0.5

[a] MIC values displayed in  $\mu\text{g mL}^{-1}$  and measured in lysogeny broth (LB) supplemented with 0.3 mM ZnSO<sub>4</sub>.

addition to the published conditions, a variety of other common coupling agents were also explored and found to give similar scrambling. This led us ultimately to investigate the use of the milder peptide coupling agent COMU, a uronium salt derived from Oxyma.<sup>[23]</sup> A key advantage of COMU over other peptide coupling reagents is that it incorporates a hydrogen bond accepting oxygen atom in its iminium moiety, allowing for the use of a single equivalent of base. Gratifyingly, when paired with the sterically hindered 2,2,6,6-tetramethylpiperidine (TMP), COMU was found to be very effective at suppressing base-promoted epimerisation. This was reflected in the marked decrease in the formation of the BacA<sub>A</sub> and BacA<sub>C</sub> diastereomers as evidenced by HPLC analysis of the crude product. This further supports the notion the undesired BacA<sub>A</sub> and BacA<sub>C</sub> diastereomers correspond to bacitracin A variants bearing the incorrect *S*-configuration at the Cys2  $\alpha$ -position of the thiazoline moiety. Collectively, the use of COMU/TMP for the coupling of thiazoline 5, along with the optimised cleavage and deprotection conditions, resulted in effective suppression of the unwanted diastereomers. Compared to the previously published route which yields a mixture of four bacitracin diastereomers in similar quantities, our optimised conditions result in the formation of bacitracin A as the major species (Scheme 2).

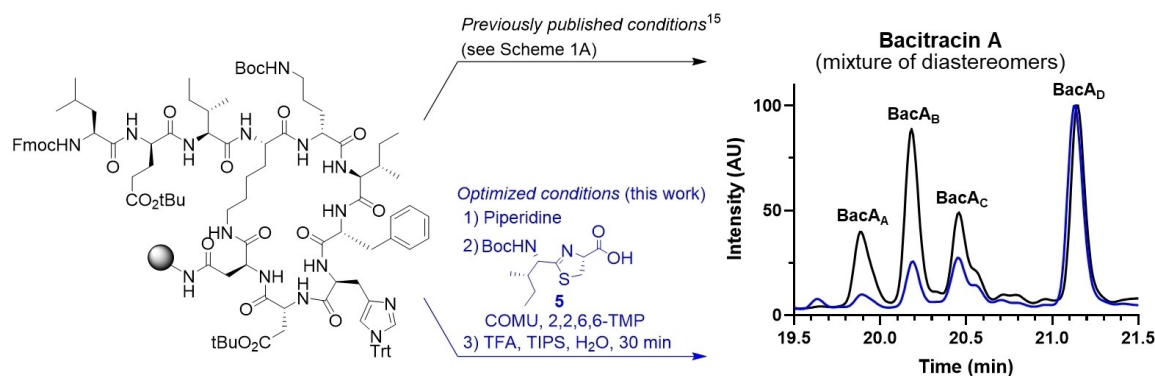
Our findings also provide insights into the relative importance of stereochemistry in bacitracin's N-terminal aminothiazoline motif. It appears that the *R*-configuration at the Cys2-derived  $\alpha$ -position is essential as the BacA<sub>A</sub> and BacA<sub>C</sub> diastereomers, both bearing an *S*-configuration at this position, are devoid of activity. By comparison, the BacA<sub>B</sub> diastereomer wherein the Ile1-derived  $\alpha$ -position is inverted but the Cys2-derived  $\alpha$ -position is the same as for bacitracin A, retains some antibacterial activity, albeit much less than the natural product (Table 1). It is perhaps not surprising that the Cys2 stereocentre is more critical for antibacterial activity. As is evident in the crystal structure of bacitracin A bound to zinc and geranylpyrophosphate (Figure 1B), the sp<sup>2</sup> nitrogen of the thiazoline and adjacent N-terminal amino group are both actively involved in zinc binding. The Cys2 stereocentre plays a key role in setting the orientation of the aminothiazoline moiety and it stands to reason that the incorrect configuration at this centre would

severely impact its capacity to contribute to the zinc chelation essential to bacitracin's activity.

## Exploring alternative zinc binding motifs

The challenges associated with the synthesis and coupling of the aminothiazoline moiety, as well as its established role in the systemic toxicity of bacitracin A,<sup>[4,9]</sup> prompted us to explore alternative zinc binding motifs. The crystal structure of bacitracin A bound to geranyl pyrophosphate makes clear the role played by a Zn<sup>2+</sup> ion in complexing both the antibiotic and phospholipid target, a finding that also explains the zinc-dependency of bacitracin's antibacterial activity. Another area of antibacterial research where small molecule zinc-binding compounds have recently garnered attention relates to their potential as inhibitors of zinc-dependent metallo- $\beta$ -lactamases.<sup>[24–31]</sup> Based on our experience in this regard, we therefore examined the potential for replacing the N-terminal aminothiazoline of bacitracin with alternative zinc-binding motifs such as bipyridyl and dipicolinic acid moieties. In addition, alternate dipeptides were incorporated that maintained the N-terminal Ile residue while replacing the Cys2 residue with glycine, L-alanine, or D-alanine. These analogues were prepared to probe the relative importance of the thiazoline heterocycle relative to the free N-terminal amino group. The synthesis of bacitracin analogues 6–10 followed that of bacitracin itself as outlined in Scheme 1 up to the resin-bound cyclic precursor terminating at Leu3. The alternative N-terminal groups were conveniently introduced using the corresponding carboxylic acid building blocks in the case of bipyridyl and dipicolinic acid analogues 6 and 7 respectively, while for analogues 8–10, two additional rounds of SPPS were applied to introduce the Ile-Gly, Ile-L-Ala, and Ile-D-Ala dipeptides respectively (Figure 2).

We next evaluated the antibacterial activity of bacitracin analogues 6–10 against the same panel of organisms indicated in Table 1. Unfortunately, even at the highest tested concentration of 64  $\mu$ g/mL, none of the compounds were found to be active against the Gram-positive bacterial strains screened



**Scheme 2.** Optimised synthesis conditions of bacitracin A (1) leading to the suppression of diastereomer by-products illustrated with HPLC analysis. The optimised conditions result in formation of the desired BacA<sub>D</sub> as the major species (blue trace) in contrast to the diastereomeric mixture obtained when using the previously published conditions (black trace).

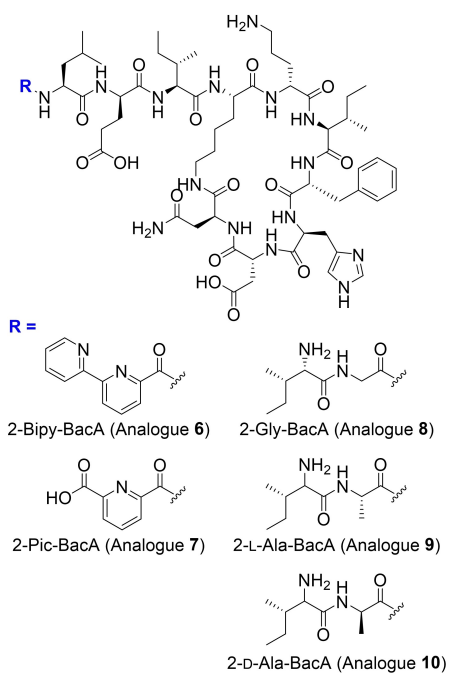


Figure 2. Structures of non-thiazoline bearing bacitracin analogues 6–10.

(Table S3). This finding is in line with our previous assessment of the bacitracin A BacA<sub>A-C</sub> diastereomers, which revealed that the orientation of the N-terminal zinc chelating moiety is finely tuned and small variations in its positioning can lead to a precipitous loss of activity. Notably, the zinc binding motifs in analogues 6 and 7 are planar and are likely misaligned with bacitracin's zinc binding pocket. Furthermore, the lack of activity observed for analogues 8–10, makes clear the importance of the thiazoline moiety. Our findings also agree with the results of a previous study reported by Marahiel and co-workers who applied a chemoenzymatic approach to generating bacitracin A and unnatural analogues.<sup>[21]</sup> They found similarly attenuated activities for analogues bearing alternative heterocycles at the bacitracin N-terminus also pointing to the importance of the aminothiazoline moiety for antibacterial activity.

## Conclusion

In summary, we have developed an optimised protocol for the synthesis of bacitracin A that circumvents previously unaddressed stereochemical issues associated with the N-terminal aminothiazoline moiety. This optimised combined solid- and solution-phase approach, suppresses the formation of unwanted stereoisomers resulting in a higher yield and more convenient purification of the desired bacitracin A species. A series of novel bacitracin analogues were also prepared to investigate the possibility of replacing the N-terminal aminothiazoline moiety with other zinc-binding motifs and acyclic dipeptides. These new analogues were found to be inactive as antibiotics demonstrating the key role played by the amino-

thiazoline moiety. Notably, the improved synthetic route here described provides access to the bacitracin scaffold with confidence in the stereochemical purity of the product. Future work will be aimed at applying this improved route to investigate the effects of other structural variations throughout the bacitracin framework to generate new SAR insights.

## Experimental Section

All reagents employed were of American Chemical Society (ACS) grade or higher and were used without further purification unless otherwise stated. HPLC-grade acetonitrile, peptide grade *N,N*-dimethylformamide (DMF) and dichloromethane (DCM) for peptide synthesis were purchased from Biosolve Chimie SARL and VWR, respectively. Unless otherwise stated, <sup>1</sup>H NMR and <sup>13</sup>C NMR spectra were recorded on a Bruker AV-400 spectrometer. The chemical shifts are noted as  $\delta$ -values in parts per million (ppm) relative to the signal of CDCl<sub>3</sub> for <sup>1</sup>H NMR ( $\delta$ =7.26 ppm) and relative to the solvent signal of CDCl<sub>3</sub> for <sup>13</sup>C NMR ( $\delta$ =77.16 ppm). Coupling constants (*J*) are given in Hz.

**Chemical synthesis:** Compounds 3<sup>[32]</sup> and 4<sup>[33]</sup> were synthesised as previously reported, see the Supporting Information for full synthetic details.

**(R)-2-[1'(S)-(tert-Butoxycarbonylamino)-2'(S)-methylbutyl]- $\Delta^2$ -thiazoline-4-carboxylic acid (5):** To a solution of 4 (1.06 g, 3.21 mmol) in 1,2-dichloroethane (16 mL) was added trimethyltin hydroxide (1.74 g, 9.63 mmol). The solution was heated to 80 °C with stirring under an inert atmosphere for 2 hours. After full conversion by TLC, the mixture was concentrated under reduced pressure. The residue was then diluted with EtOAc (50 mL) and washed with 0.01 M KHSO<sub>4</sub> (3 × 50 mL). The pH of the combined aqueous layers was measured, and then gently acidified by dropwise addition of 1 M KHSO<sub>4</sub> until a pH of 3–4 was achieved. Next the combined aqueous layers were extracted once with EtOAc (100 mL). The combined organic layers were next washed further with 0.01 M KHSO<sub>4</sub> (3 × 150 mL) and brine (1 × 150 mL). The organic layer was dried over Na<sub>2</sub>SO<sub>4</sub>, filtered, and concentrated. For practical reasons the residue was redissolved in 1:1 tBuOH/H<sub>2</sub>O (50 mL) and lyophilised to afford 5 (0.79 g, 78%) as a white solid. <sup>1</sup>H NMR (400 MHz, CDCl<sub>3</sub>)  $\delta$  8.14 (br s, 1H, OH), 5.48 (d, *J*=8.8 Hz, 1H, NH), 5.20 (t, *J*=9.1 Hz, 1H, CHCOOH), 4.50 (s, 1H, CH), 3.65 (t, *J*=10.3 Hz, 1H, SCHH), 3.57 (t, *J*=10.3 Hz, 1H, SCHH), 1.93 (d, *J*=10.9 Hz, 1H, CH<sub>3</sub>CH), 1.48 (d, *J*=6.2 Hz, 1H, CH<sub>3</sub>CHH), 1.43 (s, 9H, C(CH<sub>3</sub>)<sub>3</sub>), 1.21–1.07 (m, 1H, CH<sub>3</sub>CHH), 0.95 (d, *J*=7.1 Hz, 3H, CHCH<sub>3</sub>), 0.90 (t, *J*=5.7 Hz, 3H, CH<sub>2</sub>CH<sub>3</sub>). <sup>13</sup>C-NMR (101 MHz, CDCl<sub>3</sub>)  $\delta$  180.6 (C), 173.0 (C), 155.8 (C), 80.4 (C), 77.2 (CH), 56.8 (CH), 38.7 (CH), 35.3 (CH<sub>2</sub>), 28.4 ((CH<sub>3</sub>)<sub>3</sub>), 26.62 (CH<sub>2</sub>), 15.7 (CH<sub>3</sub>), 11.9 (CH<sub>3</sub>). HRMS (ESI) *m/z*: [M+H]<sup>+</sup> calculated for C<sub>14</sub>H<sub>24</sub>N<sub>2</sub>O<sub>4</sub>S 317.1530 found 317.1531.

## Solid-phase peptide synthesis

**General procedure A: peptide backbone synthesis (automated):** The resin bound linear decapeptide was assembled on a CEM HT12 Liberty Blue peptide synthesiser. This commenced with Fmoc-L-Asp-Oallyl being loaded onto MBHA rink amide resin through its side chain. The linear peptide was then extended with 9 further SPPS cycles sequentially adding: Fmoc-D-Asp(tBu)-OH, Fmoc-L-His(Trt)-OH, Fmoc-D-Phe-OH, Fmoc-L-Ile-OH, Fmoc-D-Orn(Boc)-OH, Fmoc-L-Lys(Alloc)-OH, Fmoc-L-Ile-OH, Fmoc-D-Glu(tBu)-OH, and Fmoc-L-Leu-OH. This was achieved by

first swelling MBHA rink amide resin (163 mg, 0.1 mmol) in 10 mL of DMF for 5 minutes. Fmoc deprotections were carried out in a solution of piperidine in DMF (1:4 v/v, 3 mL) heated to 76 °C for 15 seconds followed by 50 seconds at 90 °C. The resin was then washed with DMF (3×2 mL). Single amino acid coupling cycles were performed in DMF (4 mL) and mediated by DIC (0.125 mol/L, 5 eq.), Oxyma (0.125 mol/L, 5 eq.) and the respective Fmoc amino acid (0.125 mol/L, 5 eq.) at 75 °C for 15 seconds followed by 110 seconds at 90 °C. The only exception was Fmoc-L-His(Trt)-OH, where the coupling was performed at 25 °C for 2 minutes followed by 8 minutes at 50 °C. After the 10<sup>th</sup> amino acid was coupled, a final washing step was performed (3×2 mL DMF). At this stage the resin bound decapeptide was removed from the peptide synthesiser, manually washed with DCM, and dried under a continuous flow of nitrogen.

**General procedure B: cyclisation (manual):** The peptide-loaded resin was swollen in DCM (*ca.* 7 mL) for 10 minutes under a nitrogen atmosphere. To this was added Pd(PPh<sub>3</sub>)<sub>4</sub> (30 mg, 0.03 mmol), phenylsilane (0.30 mL, 3.0 mmol) with a flow of nitrogen providing agitation. After 1 hour, the reaction mixture was drained thoroughly washed. Firstly, with DCM (5×10 mL), then a solution of diethyldithiocarbamic acid trihydrate sodium salt (5 mg mL<sup>-1</sup> in DMF, 5×10 mL), and finally DMF (5×10 mL). After confirmation of Alloc/Allyl deprotection by LCMS, cyclisation was achieved by treatment of the peptide with 4 equivalents of BOP and 8 equivalents of DIPEA in 4 mL of DMF for 1 hour. The resin was then washed with DMF (3×4 mL).

**General procedure C: N-terminal coupling (manual):** The terminal Fmoc group was removed with piperidine in DMF (1:4 v/v, 2×5 mL, 1×5 min, 1×15 min). The resin was then washed with DMF (3×4 mL). Next, a solution of Boc-protected amino-thiazoline building block 5 (2 eq.), COMU (2 eq.), and 2,2,6,6-tetramethylpiperidine (1 eq.) in 4 mL of DMF was allowed to react for 1 minute before being added to the resin bound cyclised decapeptide. Once the reaction was complete, visible by colour change (*ca.* 1 hour) the resin was drained and washed with DMF (3×5 mL).

**General procedure D: global deprotection and cleavage from resin:** The completed peptide was simultaneously deprotected and cleaved from the resin by treatment with a mixture of TFA : TIPS : H<sub>2</sub>O (95:2.5:2.5 v/v/v, 5 mL) for 30 minutes. The reaction mixture was filtered and added to a cooled mixture of MTBE/hexanes (1:1 v/v, 45 mL). This led to the precipitation of the peptide which was collected by centrifugation and washed twice more with MTBE/hexanes (2×50 mL), yielding crude bacitracin A.

**General procedure E: preparative HPLC purification:** Bacitracin and derivatives were purified using a BESTA-Technik system with a Dr. Maisch Reprosil Gold 120 C18 column (25×250 mm, 10 μm) and equipped with a ECOM Flash UV detector monitoring at 214 and 254 nm. As solvent system, at a flow rate of 12 mL/min, was used: solvent A (0.1% TFA in water/acetonitrile [95:5 v/v]); solvent B (0.1% TFA in water/acetonitrile [95:5 v/v]). Gradient elution was as follows: 100:0 to 40:60 A/B over 80 min, 40:60 to 0:100 A/B over 1 min, 0:100 A/B for 5 min, then reversion back to 100:0 A/B over 1 min, 100:0 A/B

for 3 min, total method = 90 min. After collection, fractions were frozen and lyophilised yielding pure peptide as a white powder.

**Bacitracin A (1):** The peptide was prepared according to the *general procedure for synthesis of bacitracin peptides* at 0.1 mmol scale. Yield: 28 mg, 20%. HRMS (ESI) m/z: (M + 2H<sup>+</sup>)/2 calculated for C<sub>66</sub>H<sub>103</sub>N<sub>17</sub>O<sub>16</sub>S 711.8818 found 711.8819. HPLC R<sub>t</sub> = 14.06 min.

**2-Bipy-BacA (analogue 6):** Rink Amide AM resin (250 mg, 0.125 mmol) was used for solid phase peptide synthesis according to general procedure A. After checking the peptide by LC-MS, the peptide was cyclised according to general procedure B. The terminal Fmoc group was then removed with piperidine in DMF (1:4 v/v, 2×5 mL, 1×5 min, 1×15 min). Next the resin bound peptide was treated a solution of [2,2'-bipyridine]-6-carboxylic acid (4 eq.), BOP (4 eq.), and DIPEA (8 eq.) in 4 mL of DMF. After 1 hour the resin was drained and washed with DMF (3×5 mL). Subsequently, the peptide was simultaneously deprotected and cleaved from resin (general procedure D) and purified by preparative HPLC (general procedure E). Yield: 44 mg, 25%. HRMS (ESI) m/z: (M + 2H<sup>+</sup>)/2 calculated for C<sub>68</sub>H<sub>95</sub>N<sub>17</sub>O<sub>16</sub> 703.8645 found 703.8649. HPLC R<sub>t</sub> = 13.22 min.

**2-Pic-BacA (analogue 7):** Rink Amide AM resin (250 mg, 0.125 mmol) was used for solid phase peptide synthesis according to general procedure A. After checking the peptide by LC-MS, the peptide was cyclised according to general procedure B. The terminal Fmoc group was then removed with piperidine in DMF (1:4 v/v, 2×5 mL, 1×5 min, 1×15 min). Next the resin bound peptide was treated a solution of 6-(((4-methoxybenzyl)oxy)carbonyl)picolinic acid<sup>[26]</sup> (4 eq.), BOP (4 eq.), and DIPEA (8 eq.) in 4 mL of DMF. After 1 hour the resin was drained and washed with DMF (3×5 mL). Subsequently, the peptide was simultaneously deprotected and cleaved from resin (general procedure D) and purified by preparative HPLC (general procedure E). Yield: 35 mg, 20%. HRMS (ESI) m/z: (M + 2H<sup>+</sup>)/2 calculated for C<sub>64</sub>H<sub>92</sub>N<sub>16</sub>O<sub>18</sub> 687.3461 found 687.3466. HPLC R<sub>t</sub> = 13.72 min.

**2-Gly-BacA (analogue 8):** Rink Amide AM resin (200 mg, 0.1 mmol) was used for solid phase peptide synthesis according to general procedure A. The linear peptide was extended by an additional 2 SPPS cycles that sequentially incorporated Fmoc-Gly-OH, and Fmoc-L-Ile-OH generating a resin-bound linear dodecapeptide. After checking the peptide by LC-MS, the peptide was cyclised according to general procedure B. The terminal Fmoc group was then deprotection with piperidine in DMF (1:4 v/v, 2×5 mL, 1×5 min, 1×15 min). Subsequently, the peptide was simultaneously deprotected and cleaved from resin (general procedure D) and purified by preparative HPLC (general procedure E). Yield: 34 mg, 24%. HRMS (ESI) m/z: (M + 2H<sup>+</sup>)/2 calculated for C<sub>65</sub>H<sub>103</sub>N<sub>17</sub>O<sub>17</sub> 697.8932 found 697.8936. HPLC R<sub>t</sub> = 12.70 min.

**2-L-Ala-BacA (analogue 9):**<sup>[21]</sup> Rink Amide AM resin (200 mg, 0.1 mmol) was used for solid phase peptide synthesis according to general procedure A. The linear peptide was extended by an additional 2 SPPS cycles that sequentially incorporated Fmoc-L-Ala-OH, and Fmoc-L-Ile-OH generating a resin-bound linear dodecapeptide. After checking the peptide by LC-MS, the

peptide was cyclised according to general procedure B. The terminal Fmoc group was then deprotection with piperidine in DMF (1:4 v/v, 2×5 mL, 1×5 min, 1×15 min). Subsequently, the peptide was simultaneously deprotected and cleaved from resin (general procedure D) and purified by preparative HPLC (general procedure E). Yield: 19 mg, 13%. HRMS (ESI) m/z: (M + 2H<sup>+</sup>)/2 calculated for C<sub>66</sub>H<sub>105</sub>N<sub>17</sub>O<sub>17</sub> 704.9010 found 704.9012. HPLC R<sub>t</sub> = 12.60 min.

**2-D-Ala-BacA (analogue 10):** Rink Amide AM resin (200 mg, 0.1 mmol) was used for solid phase peptide synthesis according to general procedure A. The linear peptide was extended by an additional 2 SPPS cycles that sequentially incorporated Fmoc-D-Ala-OH, and Fmoc-L-Ile-OH generating a resin-bound linear dodecapeptide. After checking the peptide by LC-MS, the peptide was cyclised according to general procedure B. The terminal Fmoc group was then deprotection with piperidine in DMF (1:4 v/v, 2×5 mL, 1×5 min, 1×15 min). Subsequently, the peptide was simultaneously deprotected and cleaved from resin (general procedure D) and purified by preparative HPLC (general procedure E). Yield: 41 mg, 29%. HRMS (ESI) m/z: (M + 2H<sup>+</sup>)/2 calculated for C<sub>66</sub>H<sub>105</sub>N<sub>17</sub>O<sub>17</sub> 704.9010 found 704.9012. HPLC R<sub>t</sub> = 13.13 min.

**MIC determinations:** From glycerol stocks, bacterial strains were cultured on blood agar plates and incubated overnight at 37 °C. Following incubation, 3 mL of tryptic soy broth (TSB) was inoculated with an individual colony. The cultures were grown to exponential phase (OD<sub>600</sub> = 0.5) at 37 °C. The bacterial suspensions were then diluted 100-fold in lysogeny broth supplemented with 0.3 M ZnSO<sub>4</sub> (ZnLB) to reach a bacterial cell density of 10<sup>6</sup> CFU mL<sup>-1</sup>. In polypropylene 96-well microtiter plates, test compounds in ZnLB were added in triplicate and 2-fold serially diluted to achieve a final volume of 50 μL per well. An equal volume of bacterial suspension (10<sup>6</sup> CFU mL<sup>-1</sup>) was added to the wells. The plates were sealed with breathable membranes and incubated at 37 °C for 18 h with constant shaking (600 rpm). MICs were determined by visual inspection as the median of a minimum of triplicates.

## Acknowledgements

Financial support provided by The European Research Council (ERC consolidator grant to NIM, grant agreement no. 725523).

## Conflict of Interest

The authors declare no conflict of interest.

## Data Availability Statement

The data that support the findings of this study are available in the supplementary material of this article.

**Keywords:** antibiotics · antibiotic resistance · bacitracin · natural products · peptide synthesis · thiazoline

- [1] C. J. L. Murray, et al. *Lancet* **2022**, 399, 629–655.
- [2] T. Roemer, C. Boone, *Nat. Chem. Biol.* **2013**, 9, 222–231.
- [3] M. N. Gwynn, A. Portnoy, S. F. Rittenhouse, D. J. Payne, *Ann. N. Y. Acad. Sci.* **2010**, 1213, 5–19.
- [4] V. Pavli, V. Kmetec, *J. Pharm. Biomed. Anal.* **2001**, 24, 977–982.
- [5] B. A. Johnson, H. Anker, F. L. Meloney, *Science* **1945**, 102, 376–377.
- [6] G. Drapeau, E. Petitclerc, A. Toulouse, F. Marceau, *Antimicrob. Agents Chemother.* **1992**, 36, 955–961.
- [7] L. J. Ming, J. D. Epperson, *J. Inorg. Biochem.* **2002**, 91, 46–58.
- [8] D. Konz, A. Klens, K. Schorgendorfer, M. A. Marahiel, *Chem. Biol.* **1997**, 4, 927–937.
- [9] S. A. Suleiman, F. Song, M. Su, T. Hang, M. Song, *J. Pharm. Anal.* **2017**, 7, 48–55.
- [10] G. Siwert, J. L. Strominger, *Proc. Natl. Acad. Sci. USA* **1967**, 57, 767–773.
- [11] K. J. Stone, J. L. Strominger, *Proc. Natl. Acad. Sci. USA* **1971**, 68, 3223–3227.
- [12] D. R. Storm, J. L. Strominger, *J. Biol. Chem.* **1973**, 248, 3940–3945.
- [13] D. R. Storm, *Ann. N. Y. Acad. Sci.* **1974**, 235, 387–398.
- [14] N. J. Economou, S. Cocklin, P. J. Loll, *Proc. Natl. Acad. Sci. USA* **2013**, 110, 14207–14212.
- [15] J. Lee, J. H. Griffin, T. I. Nicas, *J. Org. Chem.* **1996**, 61, 3983–3986.
- [16] C. Pan, T. Kuranaga, H. Kakeya, *Org. Biomol. Chem.* **2020**, 18, 8366–8370.
- [17] K. C. Nicolaou, A. A. Estrada, M. Zak, S. H. Lee, B. S. Safina, *Angew. Chem. Int. Ed.* **2005**, 44, 1378–1382; *Angew. Chem.* **2005**, 117, 1402–1406.
- [18] Y. Ken, H. Yoshihiro, S. Tetsuo, *Bull. Chem. Soc. Jpn.* **1975**, 48, 3302–3305.
- [19] Y. Hirotsu, T. Shiba, T. Kaneko, *Bull. Chem. Soc. Jpn.* **1970**, 43, 1870–1873.
- [20] A. C. Gaumont, M. Gulea, J. Levillain, *Chem. Rev.* **2009**, 109, 1371–1401.
- [21] B. Wagner, D. Schumann, U. Linne, U. Koert, M. A. Marahiel, *J. Am. Chem. Soc.* **2006**, 128, 10513–10520.
- [22] W. Konigsberg, R. J. Hill, L. C. Craig, *J. Org. Chem.* **1961**, 26, 3867–3871.
- [23] R. Subiros-Funosas, L. Nieto-Rodriguez, K. J. Jensen, F. Albericio, *J. Pept. Sci.* **2013**, 19, 408–414.
- [24] K. Tehrani, N. I. Martin, *ACS Infect. Dis.* **2017**, 3, 711–717.
- [25] K. Tehrani, N. C. Bruchle, N. Wade, V. Mashayekhi, D. Pesce, M. J. van Haren, N. I. Martin, *ACS Infect. Dis.* **2020**, 6, 1366–1371.
- [26] M. J. van Haren, K. Tehrani, I. Kotsogianni, N. Wade, N. C. Bruchle, V. Mashayekhi, N. I. Martin, *Chem. Eur. J.* **2021**, 27, 3806–3811.
- [27] N. Wade, K. Tehrani, N. C. Bruchle, M. J. van Haren, V. Mashayekhi, N. I. Martin, *ChemMedChem* **2021**, 16, 1651–1659.
- [28] K. Tehrani, H. Fu, N. C. Bruchle, V. Mashayekhi, A. Prats Lujan, M. J. van Haren, G. J. Poelarends, N. I. Martin, *Chem. Commun.* **2020**, 56, 3047–3049.
- [29] H. Zhang, K. Yang, Z. Cheng, C. Thomas, A. Steinbrunner, C. Pryor, M. Vulcan, C. Kemp, D. Orea, C. Paththamperuma, A. Y. Chen, S. M. Cohen, R. C. Page, D. L. Tierney, M. W. Crowder, *Bioorg. Med. Chem.* **2021**, 40, 116183.
- [30] K. Tehrani, N. Wade, V. Mashayekhi, N. C. Bruchle, W. Jespers, K. Voskuil, D. Pesce, M. J. van Haren, G. J. P. van Westen, N. I. Martin, *J. Med. Chem.* **2021**, 64, 9141–9151.
- [31] A. Y. Chen, P. W. Thomas, A. C. Stewart, A. Bergstrom, Z. Cheng, C. Miller, C. R. Bethel, S. H. Marshall, C. V. Credille, C. L. Riley, R. C. Page, R. A. Bonomo, M. W. Crowder, D. L. Tierney, W. Fast, S. M. Cohen, *J. Med. Chem.* **2017**, 60, 7267–7283.
- [32] M. Toumi, F. Couty, G. Evano, *J. Org. Chem.* **2008**, 73, 1270–1281.
- [33] M. North, G. Pattenden, *Tetrahedron* **1990**, 46, 8267–8290.

Manuscript received: September 18, 2022

Revised manuscript received: October 26, 2022

Accepted manuscript online: October 26, 2022

Version of record online: November 18, 2022